2-[(4-Azido-2-nitrophenyl)amino]ethyl Triphosphate, a Novel Chromophoric and Photoaffinity Analogue of ATP. Synthesis, Characterization, and Interaction with Myosin Subfragment 1†

Kay L. Nakamaye,‡ James A. Wells,§ Robert L. Bridenbaugh,§ Yoh Okamoto,‖ and Ralph G. Yount*

Biochemistry/Biophysics Program, Institute of Biological Chemistry, and Department of Chemistry, Washington State University, Pullman, Washington 99164

Received January 22, 1985

ABSTRACT: A facile and high-yield synthesis of a new ATP analogue, 2-[(4-azido-2-nitrophenyl)amino]ethyl triphosphate (NANTP), is described. NANTP and ATP are hydrolyzed by skeletal myosin subfragment 1 (SF_1) at comparable rates in the presence of Ca^{2+}, Mg^{2+}, or NH_4^+-EDTA. NANTP is also cleaved but less readily by mitochondrial F_1-ATPase and by ($Na^+ + K^+$)-ATPase from dog brain and hog kidney. F-Actin markedly activates NANTP cleavage by SF_1 in the presence of Mg^{2+}, suggesting that the diphosphate product NANDP is slow to be released from the enzyme. [α-^{32}P]NANDP binds to a single site on SF_1 ($K_A = 1 \times 10^6$ M^{-1}) with an affinity identical with that of ADP. The absorption maximum of NANDP was shifted from 474 to 467 nm upon binding to SF_1, suggesting that the purine binding site has a dielectric constant of about 45. NANDP was trapped in nearly stoichiometric amounts at the active site by cross-linking SH_1 and SH_2 with *N,N'-p*-phenylenedimaleimide (pPDM) or by chelation with cobalt(III) phenanthroline [Wells, J., & Yount, R. (1979) *Proc. Natl. Acad. Sci. U.S.A. 76*, 4966]. The trapped [β-^{32}P]NANDP·SF_1 complex, like the comparable ADP·SF_1 complex, was stable for days at 0 °C and could be purified free of extraneous analogue by ammonium sulfate precipitation and gel filtration. Photolysis of the purified complex gave >50% covalent incorporation of the trapped NANDP into the 95-kilodalton (kDa) heavy chain of SF_1. Limited trypsinization and analysis by gel electrophoresis showed that >95% of the bound label was associated with the 25-kDa NH_2-terminal peptide. Without trapping, NANDP labeling of SF_1 was nonspecific and was not prevented by addition of a large excess of ATP. This new approach of trapping photoaffinity analogues by cross-linking agents before photolysis may prove to be of general usefulness in increasing the specificity and extent of labeling of enzymes that undergo substrate-induced conformation changes.

Knowledge of the structural characteristics of the adenosinetriphosphatase (ATPase) site of myosin is essential for an understanding of force generation in muscle contraction. Attempts to identify this site by covalent affinity labels (Haley & Yount, 1971; Wagner & Yount, 1976; Togashi & Reisler, 1982) or by ligand exchange into substitution-inert metal ion–ATP complexes (Werber et al., 1974; Wells et al., 1980b) have been largely unsuccessful. The most promising approach appears to be the use of various photoaffinity analogues of ATP. Guillory & Jeng (1977) have described the synthesis of a series of ATP analogues in which a nitrophenyl azide moiety is attached with varying length linker groups to the 3'-OH of ribose of ATP. They showed that the analogue with a β-alanyl linker group photoinactivated myosin in the absence but not in the presence of ATP (Jeng & Guillory, 1975). Szilagyi et al. (1979) subsequently showed that this analogue labeled predominantly the 25-kDa NH_2-terminal tryptic peptide of the heavy chain fragment of SF_1.[1] Thus it appears that a peptide (or peptides) within 10 Å [i.e., the span of an *N*-(2-nitro-4-azidophenyl)-β-alanine grouping] of the ribose ring of ATP can be identified with this analogue.

Direct photolysis of ATP or UTP has also been effective in labeling the heavy chains of myosin from *Acanthamoeba* and turkey gizzard (Maruta & Korn, 1981). Rabbit skeletal myosin SF_1, however, was labeled less than 1% by the same technique. Moreover, skeletal myosin in our hands (R. Bridenbaugh, unpublished results) is extremely sensitive to the short-wavelength irradiation necessary in such an approach, an observation that brings into question the specificity of any direct photolabeling that might occur with ATP.

To overcome the above handicap and to define further the active site of myosin, we have prepared a new photoaffinity analogue of ATP, NANTP (Figure 1). The (nitroaryl)azido group of this analogue is known to be readily photolyzed by visible light (Fleet et al., 1969), thus avoiding the sensitivity of myosin to UV light. In addition, the aromatic ring should bind at or near the purine binding site on myosin, yielding more specific information about the active site than previous photoaffinity labeling studies. This report describes the synthesis and properties of NANTP and NANDP and details their use as reversible probes of the active site of myosin under conditions of low light. Despite its relatively simple structure,

† Supported by grants from the NIH (AM 05195), the Muscular Dystrophy Association, and the American Heart Association.

‡ NSF Science Faculty Professional Development Awardee. Permanent address: Department of Chemistry, Gonzaga University, Spokane, WA.

§ Present address: Genentech, South San Francisco, CA.

‖ Postdoctoral Fellow of the Muscular Dystrophy Association. Present address: Department of Biochemistry, Juntendo University, Tokyo, Japan.

[1] Abbreviations: NAN, 2-[(4-azido-2-nitrophenyl)amino]ethanol; NANMP, NANDP, and NANTP, mono-, di-, and triphosphate esters of NAN; ADP and ATP, adenosine 5'-di- and triphosphate; SF_1, myosin subfragment 1; HMM, heavy meromyosin; AMP-PNP, 5'-adenylyl imidodiphosphate; HMPA, hexamethylphosphoramide; Bu_3N, tributylamine; pPDM, *N,N'-p*-phenylenedimaleimide; phen, 1,10-phenanthroline; oPDM, *N,N'-o*-phenylenedimaleimide; F_2DPS, 4,4'-difluoro-3,3'-dinitrophenyl sulfone; DTNB, 5,5'-dithiobis(2-nitrobenzoic acid); EDTA, ethylenediaminetetraacetic acid; Tris, tris(hydroxymethyl)aminomethane.

0006-2960/85/0424-5226$01.50/0

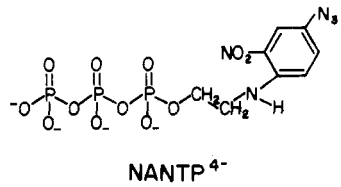

NANTP^{4-}

FIGURE 1: Structure of NANTP.

NANTP has proven to be remarkably similar to ATP in its interactions with myosin and muscle fibers. In work to be published elsewhere (R. Bridenbaugh et al., unpublished results), NANTP is shown to support contraction and relaxation of chemically skinned muscle fibers in a manner completely analogous to ATP. This is good evidence that the nitroaryl azide ring of NANTP binds to myosin where the adenine ring of ATP normally binds.

NANDP was also found to be trapped at the active site of SF_1 by a variety of dithiol cross-linking agents in a manner identical with that observed previously for ADP [Wells & Yount, 1979; Wells et al., 1980a,c; for a review, see Wells & Yount (1982)]. The trapped NANDP·SF_1 complex is remarkably stable ($t_{1/2}$ > 5 days at 0 °C) and can be purified free of nontrapped NANDP by conventional ammonium sulfate precipitation and gel filtration. Irradiation of the purified complex then assured that only residues at the active site would be labeled. This approach was essential to obtain specific and high levels of covalent labeling of myosin. Without prior trapping, photolabeling required large excesses of NANDP and was highly nonspecific. In this paper, NANDP trapped on SF_1 is shown to label specifically the 25-kilodalton (kDa) NH_2-terminal tryptic peptide,[2] a fragment previously proposed by Szilagzi et al. (1979) to contain the ATP binding site.

Materials and Methods

Sodium salts of ATP and ADP were from P-L Biochemicals. [2,8-^{3}H]AMP-PNP and sodium [^{32}P]orthophosphate were from ICN. 4-Fluoro-3-nitrophenyl azide was prepared as described by Guillory & Jeng (1977) and was identical with the same compound purchased from the Pierce Chemical Co. 1,1′-Carbonyldiimidazole and hexamethylphosphoramide were from Aldrich. pPDM, oPDM, and 1,10-phenanthroline were from Aldrich; F_2DPS and DTNB were from Pierce. [Co^{III}-$(phen)_2CO_3$]Cl was prepared according to Ablov & Palade (1961) as previously described (Wells et al., 1979). Preparation of triethylammonium bicarbonate solutions, synthesis of nonradioactive AMP-PNP, and analyses for total phosphate and acid-labile phosphate were as described (Yount et al., 1971). The (Na^+ + K^+)-ATPase preparations were from Sigma. F_1-ATPase was a generous gift of Dr. Harvey Penefsky.

Rabbit skeletal myosin and actin were prepared according to Wagner & Yount (1975) and Spudich & Watt (1971), respectively. SF_1 was prepared as described by Weeds & Taylor (1975) except the myosin stored in 50% glycerol at −20 °C was dialyzed directly against 50 volumes of 10 mM phosphate buffer, pH 7.0, containing 0.1 M NaCl at 4 °C prior to digestion with α-chymotrypsin in the presence of 1 mM EDTA. SF_1 was assumed to have M_r 115 000 and $\epsilon_{280}^{1\%}$ = 7.5 cm^{-1} (Wagner & Weeds, 1977). Protein concentrations of SF_1 were determined by the dye binding assay of Bradford (1976). The diluted dye reagent was allowed to stand for at least 2 h at 4 °C and was filtered through a fiberglass prefilter plus two stacked Millipore filters (1.2 and 0.45 μm) before being used. ATPase activities were measured as described (Wells et al., 1979) except that the Ca^{2+} concentration was 5 mM to avoid precipitation of CaNANTP. All experimental procedures involving the synthesis or characterization of NAN compound were carried out in the dark or under subdued light conditions. Spectra (UV–visible) were obtained on a Varian Superscan spectrophotometer. Magnesium analysis was carried out by atomic absorption with a Perkin-Elmer 360 as described (Wells et al., 1980a).

Preparation of 2-[(4-Azido-2-nitrophenyl)amino]ethanol (NAN). To a solution of 1.0 g (5.5 mmol) of 4-fluoro-3-nitrophenyl azide in 5 mL of 80% dimethylformamide was added 0.67 g (11 mmol) of redistilled ethanolamine. The resultant solution immediately turns dark red and was stirred at room temperature overnight. The solvent was removed on a rotary evaporator at 30 °C, and the reddish orange solid remaining was suspended in 10 mL of cold water and filtered to remove residual ethanolamine. The solid 2-[(4-azido-2-nitrophenyl)amino]ethanol was dissolved in warm methanol and on standing at 4 °C the solution yielded deep red crystalline platelets. Rapid cooling will yield orange-red needle-like crystals: overall yield, 85–90%; mp 96–98 °C (uncor); IR (principal λ_{max}^{KBr}) 3470 (OH), 3330 and 1500 (NH), 2090 (N_3), and 1550 and 1350 (NO_2) cm^{-1}; UV (water, pH 7) λ_{max} 262 nm (ϵ_M = 31 400 M^{-1} cm^{-1}) and 474 (5100); NMR ($DCCl_3$) 3.61 (triplet, 2 H), 4.02 (triplet, 2 H), 7.02 (multiplet, 2 H), and 7.92 (doublet, 1 H) ppm. Anal. Calcd for $C_8H_9O_3N_5$ (M_r 223): C, 43.0; H, 4.03; N, 31.4. Found: C, 42.9; H, 3.99; N, 31.1.

Preparation of NANMP. The phosphorylation of NAN followed the general procedure of Yoshikawa et al. (1967). A solution of 0.8 mL (8.6 mmol) of freshly distilled $POCl_3$[3] in 7 mL of redistilled triethyl phosphate (stored over 4-Å molecular sieves) was cooled in an ice bath. The solution was stirred vigorously while 0.90 g (4 mmol) of NAN was added slowly in small quantities. The reaction was allowed to proceed for 18 h at 0 °C after which time unreacted $POCl_3$ was removed by rotary evaporation at 30 °C. While the solution was vigorously stirred at 0 °C (ice bath), 5 mL of 4 N NaOH was added dropwise to hydrolyze the acid chlorides. Water (40 mL) was added, and the solution was allowed to stand for 2 h at 0 °C to allow unreacted NAN to come out of solution. The mixture was centrifuged at low speed to pellet NAN, and the aqueous phase containing the product was decanted and adjusted to pH 8 with either HCl or NH_4OH as required. This solution was applied to a DEAE-Sephadex (A-25) column (2.5 × 70 cm) and eluted with a linear 0–0.5 M (pH 7.6) triethylammonium bicarbonate gradient (total volume = 6 L) at 4 °C. Precipitation of a small amount of the reaction mixture permanently stained the DEAE-Sephadex at the top of the column. The elution profile monitored by absorbance at 474 nm showed a small quantity of unreacted starting material present in the void volume while the major peak of NANMP eluted at 0.3 M buffer. Two smaller unidentified products eluted at 0.4 and 0.46 M buffer, respectively. After removing the triethylammonium bicarbonate by rotary evaporation, the product, NANMP, was precipitated as the sodium salt by using 1 M NaI in acetone as described previously

[2] Sequence analysis (Tong & Elzinga, 1983) has established the true molecular weight of the 25-kDa NH_2-terminal peptide to be 23 000. We have used the 25-kDa designation in this paper for ease of reference to earlier work.

[3] It was noted that older phosphorus oxychloride samples, even if redistilled, would give multiple products and low yields at this step. The best procedure is to use freshly opened and freshly distilled $POCl_3$.

(Yount et al., 1971). Analysis of the total phosphate compared to the absorption at 474 nm gave a 1:1 molar ratio of phosphate to the nitroazidophenyl group. The spectral properties were essentially identical with those of NAN. Yields averaged 60% for five preparations.

Preparation of NANDP and NANTP. The di- and triphosphate derivatives of NAN were prepared by coupling 1,1′-carbonyldiimidazole-activated NANMP to phosphate or pyrophosphate, respectively, by the general procedures of Hoard & Ott (1975) and Ott et al. (1977). The tributylammonium salts of NANMP and pyrophosphate were prepared by passage of their sodium salts through Dowex 50 columns (H^+ form, 50–100 mesh, 10–20-fold excess capacity for Na^+) at 0–4 °C and collecting the eluant directly into vigorously stirred redistilled tributylamine (slight excess over the H^+ produced). When inorganic phosphate (P_i) was used, phosphoric acid (85%) was weighed out and neutralized with tributylamine dissolved in methanol. Water was removed in each case by repeated dissolutions in anhydrous methanol (stored over 4-Å molecular sieves) and rotary evaporation. In most cases NANMP was isolated directly as the triethylammonium salt after column purification on DEAE-Sephadex as described above and converted into the tributylammonium salt by evaporation of triethylamine after addition of excess tributylamine. In a typical synthesis, a solution of 1.0 mmol of dried NANMP (tributylammonium salt) in 5 mL of freshly distilled HMPA was stirred while 0.81 g (5.0 mmol) of 1,1′-carbonyldiimidazole dissolved in 25 mL of HMPA was added under argon gas. The reaction was allowed to proceed for 18 h under argon, and excess 1,1′-carbonyldiimidazole was destroyed by addition of 4.0 mmol of methanol with stirring for 1 h. This solution was added dropwise with mixing to 5.0 mmol of the tributylammonium salt of inorganic pyrophosphate (PP_i) dissolved in 25 mL of HMPA. After standing overnight, the reaction mixture was diluted slowly with 25 mL of water at 0 °C. The pH was adjusted to 7.5 by use of concentrated ammonium hydroxide (~0.3 mL) and the HMPA removed by extraction with 100 mL of chloroform. The chloroform layer was back-extracted twice with water, and all of the aqueous solutions were pooled and concentrated to about 40 mL on a rotary evaporator. This aqueous solution was applied on a 2.5 × 70 cm DEAE-Sephadex A-25 column, and the products were eluted with a linear 0–1.0 M triethylammonium bicarbonate buffer gradient (total volume = 6 L) at 4 °C. The elution profile was virtually free of any unreacted NANMP with less than 10% NANDP and the remainder NANTP. These compounds eluted at 0.3, 0.45, and 0.55 M buffer, respectively. The fractions containing NANTP were pooled, and triethylammonium bicarbonate was removed by repeated dissolution in methanol followed by flash evaporation at 25 °C. NANTP was isolated as the sodium salt as described for NANMP. The overall yields averaged 60–70%. Acid-labile and total phosphate analyses for NANTP gave values of 2 ± 0.05 and 3.0 ± 0.1 phosphates per NAN chromophore for four preparations, indicating the absence of inorganic polyphosphate impurities. Comparable syntheses of NANDP using NANMP and P_i gave yields of 70–80% and acid-labile to total phosphate ratios of 1.0 ± 0.05 to 2.0 ± 0.09 on the basis of $\epsilon_M = 5100\ M^{-1}\ cm^{-1}$ at 474 nm for NAN. The absorption spectra of NANDP and NANTP were virtually identical with that of NAN. [β-^{32}P]NANDP was prepared on a 40-μmol NANMP scale by using [^{32}P]P_i and the appropriately scaled-down procedure described above. The reaction mixture was chromatographed on a 1.5 × 60 cm DEAE-Sephadex A-25 column using a 0.25–0.85 M linear gradient of triethylammonium bicarbonate buffer (2 L total volume), and [β-^{32}P]NANDP was isolated as described above.

Table I: Cleavage of NANTP by SF_1 and Other ATPases[a]

assay system	μmol of P_i min^{-1} mg^{-1}		activity ratios
	NANTPase	ATPase	(NANTPase/ATPase)
subfragment 1			
NH_4^+-EDTA	4.8	13.7	0.35
Ca^{2+}	2.3	1.2	1.9
Mg^{2+}	0.14	0.025	5.6
Mg^{2+} + F-actin	1.50	0.95	1.6
(Na^+ + K^+)-ATPase			
dog kidney	0.015	0.39	0.038
cerebral cortex	0.0035	0.33	0.011
F_1-ATPase	1.79	13.3	0.075

[a] All SF_1 assays were performed at pH 8.0 at 25 °C with 6 mM ATP or NANTP. For the NH_4^+-EDTA ATPase assay, 0.2 μM SF_1, 0.56 M NH_4Cl, 0.23 M KCl, 36 mM EDTA, and 60 mM Tris hydrochloride were used. For the CaATPase assay, 1.7 μM SF_1, 5 mM $CaCl_2$, 150 mM KCl, and 180 mM Tris hydrochloride were used. For the MgATPase assay, 13 μM SF_1, 6 mM $MgCl_2$, 0.1 M KCl, and 40 mM Tris hydrochloride were used. For the actin-activated MgATPase assay, 0.77 μM SF_1, 4 μM F-actin, 6 mM KCl, 3 mM $MgCl_2$, 10 mM Tris hydrochloride, and 3 mM ATP or NANTP were used. For the (Na^+ + K^+)-ATPase assays, 14 mM KCl, 144 mM NaCl, 5 mM $MgCl_2$, 0.5 mM EDTA, 20 mM Tris, pH 7.7, and 3 mM NANTP or ATP, 37 °C, were used. For the F_1-ATPase assay, 30 mM Tris (pH 7.6), 30 mM potassium acetate, 5 mM $MgCl_2$, and 3 mM NANTP or ATP, 30 °C, were used.

The purity of each product was checked chromatographically on aluminum-backed silica gel thin-layer chromatography (TLC) plates (Merck) using isobutyric acid/concentrated NH_4OH/H_2O (66:1:33, v/v) as the developing solvent. Of several TLC solvents and media tried only this system gave consistently reproducible small spots and R_f values. The compounds with R_f values in parentheses were as follows: NAN (0.83); NANMP (0.58); NANDP (0.51); NANTP (0.45). Analysis can also be done by using the following high-performance liquid chromatography (HPLC) method: Merck trimethylammonium resin (5 μm), 30 × 0.46 cm column, solvent A = 10% EtOH, solvent B = 1 M ammonium phosphate (pH 4.1) in 10% EtOH; gradient, isocratic solvent A (0–5 min), then 5% solvent B/min to 100% solvent B (5–25 min), then isocratic solvent B (25–50 min); flow rate, 1.5 mL/min; elution times, 29 min (NANMP), 35 min (NANDP), 41 min (NANTP). Further confirmation of the structure was shown by the change in the spectrum of NANMP after photolysis (data not shown).

Enzyme Photoinactivations and Enzyme Derivatives. In a typical photoinactivation study, 1 mL of 3–15 μM SF_1 in 0.1 M KCl and 50 mM Tris, pH 8.0, buffer containing 5 mM $MgCl_2$ was mixed with varying quantities of NANDP. Samples were photolyzed in Pyrex-covered petri dishes (sample depth was 2–8 mm) on ice, 8–10 cm from a high-intensity 450-W mercury light source (Hanovia, Ace Glass), in cycles of 10-s exposure to light followed by 10-s darkness to minimize heating effects. Cross-linked enzyme derivatives containing trapped MgNANDP were prepared and purified essentially as described for MgADP complexes by Wells & Yount (1979, 1982) (see also figure and table legends).

Results

NANTP was tested as a substrate for SF_1 in the presence of various cations. As shown in Table I, NANTP was hydrolyzed at velocities that were 0.35, 1.9, and 5.6 times those of ATP in the NH_4^+-EDTA, Ca^{2+}, and Mg^{2+} assays, respectively. Similar activities were observed with only 3 mM

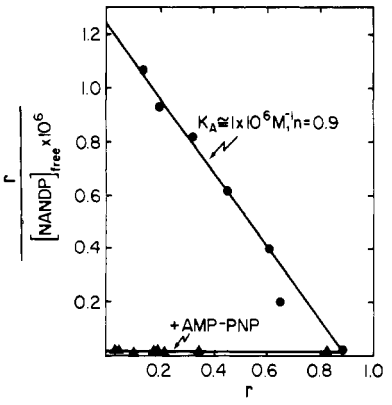

FIGURE 2: Scatchard plots for the binding of [β-^{32}P]NANDP to SF_1 in the absence (●) or presence (▲) of 0.1 mM AMP-PNP. Equilibrium dialysis was performed essentially as described by Wells & Yount (1979). Split cells (2.4 mL total volume) contained on one side 16 μM SF_1 and on both sides 20 mM $MgCl_2$, 0.1 mM KCl, 50 mM Tris, pH 8.0, and varying amounts of [β-^{32}P]NANDP. Cells were gently agitated for 36 h at 4 °C after which time solutions on each side of the cells were analyzed for ^{32}P and protein as described under Materials and Methods. r is moles of [β-^{32}P]NANDP bound per mole of SF_1.

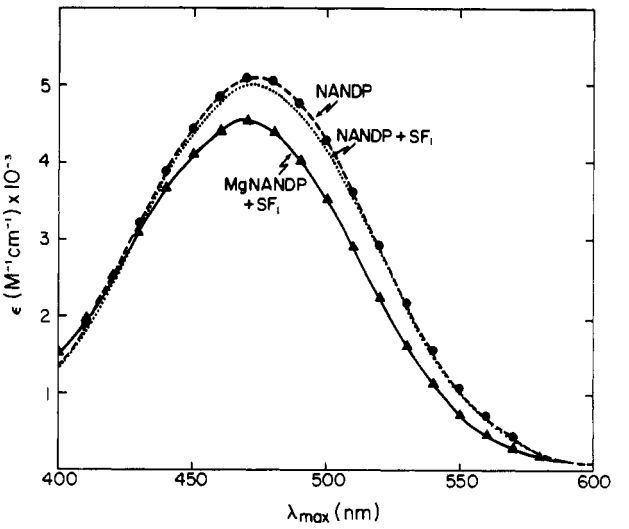

FIGURE 3: Spectra of 7.5 μM NANDP in the absence of SF_1 (●), in the presence of 16 μM SF_1 and 16 μM EDTA (···), or in the presence of 16 μM SF_1, 16 μM EDTA, and 5 mM $MgCl_2$ (▲). All spectra were recorded on a Varian Superscan spectrophotometer using a 10-cm path-length quartz cell in buffer containing 0.1 M KCl and 50 mM Tris, pH 8.2, at 25 °C. For ease in identification, symbols are placed every 10 nm on the spectra of NANDP and MgNANDP·SF_1.

NANTP or ATP, indicating the velocities given are good approximations of the V_{max} under these conditions. Interestingly, the addition of F-actin increased the MgNANTPase and MgATPase activities to almost identical values. It is well-known that the effect of F-actin binding to SF_1 is to increase the off-rate of MgADP, the normal rate-limiting step of MgATPase activity. It appears as if the release of MgNANDP is also rate limiting in MgNANTPase activity, and this suggests that NANDP and ADP bind to SF_1 in a similar manner.

The ability of NANTP to serve as an ATP-like substrate for myosin suggested it might also be cleaved by other energy-transducing enzymes. Table I also shows that NANTP is cleaved by mitochondrial F_1-ATPase and by kidney and brain (Na^+ + K^+)-ATPases. The relative rates of NANTP/ATP cleavage were as follows: F_1-ATPase, 7.5%; kidney (Na^+ + K^+)-ATPase, 4%; brain (Na^+ + K^+)-ATPase, 1%. Because of the lower rates of cleavage, a 10-fold greater enzyme concentration was used in the NANTP experiments in each case. Both the kidney and the brain ATPases were crude preparations, and it is possible other enzymes may have catalyzed cleavage of NANTP. The F_1-ATPase, however, was pure, and it cleaved NANTP at an appreciable rate. The measured F_1-ATPase activity was lower than normally reported since no ATP regenerating system was used (Gresser et al., 1982). In our hands, NANDP was not an effective substrate for the two most common ATP regenerating enzymes, i.e., creatine kinase and pyruvate kinase. NANTP also was less than 1% as active as ATP in the hexokinase-catalyzed phosphorylation of glucose. Initially it appears NANTP will be most useful as a substrate for energy-transducing ATPases and will be less effective for the various soluble kinases. Whether NANTP would be a competitive inhibitor of the latter enzymes is not known.

The activation of NANTPase activity by actin suggested that NANDP and ADP bound to the active site in similar manner. To test this hypothesis, the binding of NANDP to SF_1 was investigated directly. The Scatchard plot in Figure 2 shows that [β-^{32}P]NANDP in the presence of Mg^{2+} binds to a single site on SF_1 with $K_A = 1 \times 10^6$ M^{-1}. This value is essentially identical with that for MgADP binding to SF_1 reported by Watterson et al. (1983) using equilibrium dialysis techniques under similar binding conditions. When binding studies similar to those shown in Figure 2 were done in the absence of Mg^{2+} (data not shown), the K_A decreased to 5×10^4 M^{-1}. The addition of the known competitive inhibitor AMP-PNP eliminated NANDP binding (Figure 2), giving further evidence that NANDP is binding at the active site.

Spectral Behavior of NANDP Binding of SF_1. Binding of NANDP to SF_1 resulted in characteristic changes in the visible spectrum of the 4-azido-2-nitrophenyl group of NANDP (Figure 3). When 2 equiv of SF_1 and EDTA were added to 1 equiv of NANDP, there was a slight spectral blue shift (λ_{max} 474 nm to λ_{max} 472 nm) and a small decrease in absorption intensity. Addition of an excess of Mg^{2+} caused a marked blue shift in the absorption maximum of NANDP (474 to 467 nm) and an 11% decrease in intensity. Under these conditions over 90% of the total NANDP should be bound to SF_1 according to the affinity constant determined in Figure 2. Essentially no change in the spectrum of free NANDP occurred upon addition of Mg^{2+} alone. Addition of a 10-fold excess of AMP-PNP or pyrophosphate over SF_1 to this mixture reversed the spectrum of bound NANDP (lower curve in Figure 3) to that of free NANDP (solid curve in Figure 3). Addition of a 10-fold excess of AMP over SF_1 had no effect on the spectrum of NANDP bound to SF_1. The data in Figure 3 corroborate the direct binding studies in Figure 2 which indicate that strong binding of NANDP to SF_1 is magnesium dependent and competitive with AMP-PNP. Furthermore, addition of SF_1 (performed as in Figure 3) had no effect on the spectrum of NAN (data not shown), indicating a lack of strong binding of the parent alcohol to SF_1.

To determine the physical basis for the spectral changes accompanying the binding of NANDP to SF_1, model studies were conducted in which spectra of NANDP and NAN were taken under various conditions. No change in the spectra of NANDP could be detected in H_2O when the pH was varied from 1 to 13 (data not shown). However, a large red shift in the visible absorption maximum occurred when the polarity of the medium was increased as shown in Figure 4. The absorption maximum of NANDP dissolved in H_2O to ethanol mixtures of increasing ratio (Figure 4A) showed a linear response over a 14-nm range. Essentially the same results were obtained with NAN, showing that the observed changes are

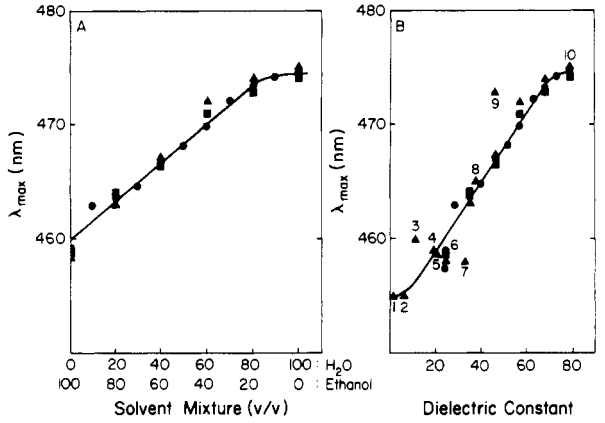

FIGURE 4: Visible absorption maxima of NANDP and NAN as a function of solvent polarity. Panel A: A 10 mM solution of NANDP (●) or NAN (▲, ■) in H_2O was diluted to 0.1 mM upon addition to the indicated H_2O/ethanol (v/v) mixtures. Spectra were recorded by use of a Varian Superscan spectrophotometer with 1-cm path-length quartz cells at 25 °C referenced against appropriate blank solutions. Panel B: Compilation of wavelength maxima for NANDP (●) and NAN (▲, ■) as a function of the dielectric constant of the medium as taken from data in panel A. In addition, 10 mM NAN in methanol was dissolved in pure solvents of varying polarity essentially as described for measurements in the H_2O/ethanol mixtures. Pure solvents (identified by numbers) were (1) dioxane, (2) ethyl acetate, (3) ethylene chloride, (4) methyl ethyl ketone, (5) acetone, (6) ethanol, (7) methanol, (8) dimethylformamide, (9) dimethyl sulfoxide, and (10) H_2O. Values of dielectric constants were taken from Landolt-Bornstein (1959).

independent of the presence of phosphate groups (Figure 4A). The absorption maximum of NANDP bound to SF_1 (467 nm) (Figure 3A) indicates a polarity of the NANDP chromophore at the active site comparable to a 40:60 H_2O:ethanol mixture. Figure 4B shows an essentially linear relationship between the dielectric constant of the medium in which the 4-azido-2-nitrophenyl group was dissolved and the observed absorption maxima. The linear relationship was roughly maintained even when solvents of radically different structure were used as shown by the numbered points in Figure 4B. NAN was employed for this latter study because it was soluble in all the solvents employed. Such dependence of the absorption maximum of a chromophore on solvent polarity is well documented (Kosower, 1958; Turner & Brand, 1968). The molar absorptivities of the NAN chromophore, however, did not show a regular dependence on solvent polarity (data not shown).

Photoinactivation of SF_1 by NANDP. Initial photoinactivation experiments were carried out with ratios of NANDP/SF_1 of 2, 25, and 50. As can be seen in Figure 5, inactivation was observed only at the higher ratios despite the fact that at the lower ratio about 75% of the SF_1 molecules should be saturated with NANDP. Most surprisingly, no protection against inactivation was provided by addition of large excesses of ATP or AMP-PNP. In fact, at the lowest NANDP to SF_1 ratio, ATP appeared to stimulate photoinactivation. Such behavior has been observed previously when addition of ATP *increased* the rate of photoinactivation of myosin by 8-azido-ATP (R. Bridenbaugh, unpublished results). Such results indicate reaction of the photoaffinity analogues with activity-critical amino acids outside the active site.

Further evidence for nonspecific labeling is given in Figure 6, which shows the covalent incorporation of [β-^{32}P]NANDP into SF_1 induced by photolysis. The inset (Figure 6) shows that incorporation of approximately three [β-^{32}P]NANDP molecules was required to inactivate SF_1 completely. The labeling in excess of the number of active sites and the fact that addition of ATP or AMP-PNP did not protect against

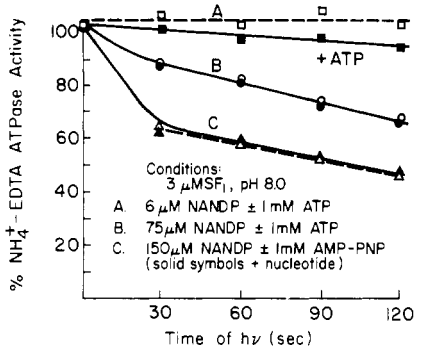

FIGURE 5: Photoinactivation of SF_1 NH_4^+-EDTA ATPase activity with NANDP in the presence or absence of ATP or AMP-PNP: SF_1 (3 μM) in KCl–Tris buffer containing 5 mM $MgCl_2$ and (curve A) 6 μM NANDP with (■) or without (□) 1 mM ATP, (curve B) 75 μM NANDP with (●) or without (○) 1 mM ATP, and (curve C) 150 μM NANDP with (▲) or without (△) 1 mM AMP-PNP. Photolysis was carried out as described under Materials and Methods. After indicated times of irradiation 50-μL aliquots were assayed for NH_4^+-EDTA ATPase activity and are reported against a nonirradiated control.

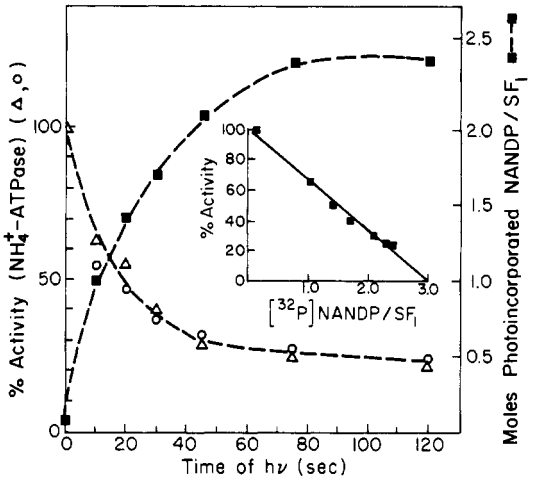

FIGURE 6: Photoincorporation of [β-^{32}P]NANDP into SF_1 during ATPase inactivation. SF_1 (15 μM) in KCl–Tris buffer containing 5 mM $MgCl_2$ and 1.5 mM [β-^{32}P]NANDP (9000 cpm/nmol) was irradiated as described under Materials and Methods. After the indicated times of irradiation aliquots were assayed for NH_4^+-EDTA ATPase activity. A parallel 0.5-mL sample was subjected to Sephadex G-25 chromatography (PD-10, Pharmacia) to remove the majority of nonbound [β-^{32}P]NANDP from SF_1. The protein concentration of the purified enzyme derivative was determined, and a 1.0-mL aliquot was precipitated by addition of 0.1 mL of 70% $HClO_4$. Following centrifugation in a Beckman microfuge the radioactivity in the protein pellet was measured to determine the amount of [β-^{32}P]NANDP photoincorporated per SF_1. The inset shows the loss of NH_4^+-EDTA ATPase activity vs. the photoincorporation of [β-^{32}P]NANDP per SF_1 from a replot of the time-dependent data.

inactivation both point to significant nonspecific labeling.

Active Site Trapping of MgNANDP. To overcome the problem of nonspecific labeling, MgNANDP was trapped at the active site by cross-linking two thiols of SF_1 by use of the reagents and procedures described previously (Wells & Yount 1979, 1982). As shown in Table II, NANDP and Mg^{2+} were trapped in nearly stoichiometric amounts by a variety of bifunctional reagents. The less than stoichiometric trapping seen here has commonly been observed with other nucleotides and reflects incomplete modification and, possibly, the presence of some inactive enzyme. As in previous experiments with ADP, NANDP appears to be trapped as the 1:1 Mg complex. The quantity of NANDP trapped could also be estimated spectrophotometrically (data not shown) by using the ab-

Table II: Trapping of Mg Complexes of NANTP and NANDP with Various Sulfhydryl Cross-Linking Reagents[a]

cross-linker	analogue	ATPase act. (% of control) NH_4^+-EDTA	ATPase act. (% of control) Ca^{2+}	trapping stoichiometry Mg/SF_1	trapping stoichiometry NANDP/SF_1
pPDM	NANTP	35		0.54	
	NANDP	32	28	0.67	
	[β-^{32}P]NANDP	14	26		0.73
	[β-^{32}P]NANDP	20	35		0.71
Co(phen)	NANTP	5	9	0.82	
	NANDP	3		0.81	
	[β-^{32}P]NANDP	6	1		0.72
	[β-^{32}P]NANDP	3			0.87
oPDM	NANTP	12	35	0.71	
	NANDP	17	16	0.64	
F_2DPS	NANTP	13		0.70	
	NANDP	11	13	0.57	
DTNB	NANTP	8	19	0.76	
	[β-^{32}P]NANDP	2	15		0.81

[a] SF_1 (15–17 μM) in 5 mM $MgCl_2$, 0.5 mM analogue, and KCl–Tris buffer, pH 8.0, at 0 °C, was inactivated by addition of one of the following cross-linking reagents: a 1.3-fold molar excess of pPDM (1 mM in acetone) for 25 min; a 10-fold molar excess of $CoCl_2$ and phen plus a 100-fold molar excess of $[Co^{III}(phen)_2CO_3]^+$ for 15 min; a 1.5-fold molar excess of oPDM for 20 min; a 1.3-fold molar excess of F_2DPS (1 mM in methanol) for 40 min or a 2-fold molar excess of DTNB (1 mM in 10 mM phosphate, pH 7.0) for 24 h. At the end of these times reaction mixtures were quenched by precipitation with 2.5 volumes of saturated $(NH_4)_2SO_4$ and 20 mM EDTA, pH 8.0. The protein pellets were collected by centrifugation, dissolved in KCl–Tris buffer, and passed over a Sephadex G-25 (PD-10) column. Final measurements of ATPase activity, protein concentration, magnesium, and ^{32}P were carried out as described under Materials and Methods. Magnesium and ^{32}P analyses were performed on separate samples to avoid having to perform atomic absorption measurements on radioactive samples.

sorption at 467 nm and assuming ϵ_M = 4540 M^{-1} cm^{-1} (see Figure 3). The values obtained were in close agreement with those determined by using [β-^{32}P]NANDP.

The characteristic spectrum of the NANDP·SF_1 complex seen in Figure 3 did not change on cross-linking with pPDM (data not shown), indicating cross-linking did not change the nature of the binding pocket. Furthermore, the addition of AMP-PNP did not change the spectrum to that of free NANDP as occurred when it was added to the un-cross-linked complex. The data in Figure 7 quantify this general effect, showing that [^{3}H]AMP-PNP did not bind to the cross-linked SF_1·NANDP complex. The small amount of binding of [^{3}H]AMP-PNP to the cross-linked complex can be explained by the presence of 6% unmodified enzyme (see inset, Figure 7).

Additional evidence that NANDP binds at the active site is shown by its ability to enhance inactivation of SF_1 by Co(phen) complexes (Table III). Previous experiments (Wells et al., 1980a) had shown that only nucleotides that are trapped at the active site will behave in this manner. Table III shows that NANDP ($t_{1/2}$ = 1.5 min) was somewhat more effective than ADP ($t_{1/2}$ = 2.0 min) in this regard. NAN, the parent alcohol, was without effect, and PP_i alone ($t_{1/2}$ = 10.6 min) was a factor of 7 less effective than NANDP, indicating that both the nitrophenyl azide ring and the pyrophosphate group were needed for optimal enhancement of inactivation and trapping.

Photoincorporation of Trapped Mg[β-^{32}P]NANDP into SF_1. The photoincorporation of Mg[β-^{32}P]NANDP trapped by Co(phen) is shown in Figure 8A. Photoincorporation was monitored by the appearance of ^{32}P in the $HClO_4$ protein pellet and by the disappearance of ^{32}P from the $HClO_4$ supernatant. The incorporation of [β-^{32}P]NANDP saturated after ap-

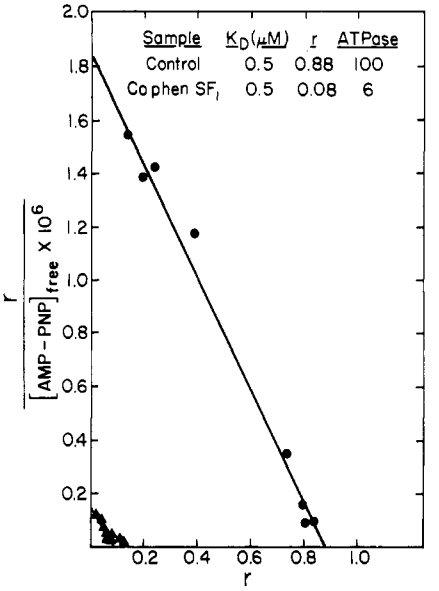

FIGURE 7: Scatchard plot showing the binding of [^{3}H]AMP-PNP to the Co(phen) cross-linked SF_1·NANDP complex. The Co(phen) SF_1·NANDP complex was prepared and purified as described under Materials and Methods by using 5 mM $MgCl_2$ and 0.5 mM NANDP. Equilibrium dialysis was performed in 2.4-mL split cells containing 16 μM SF_1 (●) or Co(phen) SF_1·NANDP (▲) on one side and 20 mM $MgCl_2$ and KCl–Tris buffer and varying amounts of [2,8-^{3}H]-AMP-PNP (5300 cpm/nmol) on both sides. Cells were gently agitated at 4 °C for 44 h and analyzed for bound and free [^{3}H]AMP-PNP. The insert table summarizes the data from the binding study, where r is the moles of [^{3}H]AMP-PNP bound per mole of SF_1.

Table III: Enhancement of NH_4^+-EDTA ATPase Inactivation by NANDP and Related Compounds[a]

compd added (5 mM)	$t_{1/2}$[b] (min)
none	20
NAN	21.8
pyrophosphate	10.6
ADP	2.0
NANDP	1.5

[a] SF_1 (15–18 μM) in 20 mM $MgCl_2$ and KCl–Tris buffer, pH 8.0 at 0 °C, was incubated with a 10-fold excess of $CoCl_2$ and 1,10-phenanthroline and a 50-fold excess of $[Co^{III}(phen)_2CO_3]^+$. [b] Half-times for NH_4^+-EDTA ATPase inactivation were determined from semilog plots of the percent residual activity vs. time. Except for occasional short lags in inactivation, plots were linear for more than three half-lives.

proximately 150 s of illumination, with nearly 60% of the trapped [β-^{32}P]NANDP becoming covalently bound. The small amount of incorporation into the once washed $HClO_4$ pellet observed before illumination (~8%) was most likely due to adventitious trapping of free [^{32}P]NANDP in the protein pellet since multiple washings reduced the background to below 3%. The spectral changes at 465 and 550 nm that accompanied the photolysis of trapped NANDP (Figure 8B) could also be used to follow the time course of the reaction, and they paralleled the pattern of radiolabeling. An almost identical time course and extent of labeling were observed when pPDM-cross-linked SF_1·NANDP was photolyzed (data not shown). Again some 55–60% of the trapped NANDP was covalently incorporated with similar accompanying spectral changes, indicating that the nature of the cross-linker does not significantly affect the photolabeling event.

Further evidence that the photoincorporation of trapped NANDP was at the active site is given in Table IV. Here [β-^{32}P]NANDP was trapped in two different SF_1 preparations by oxidizing SH_1 and SH_2 to a disulfide with a 2-fold excess

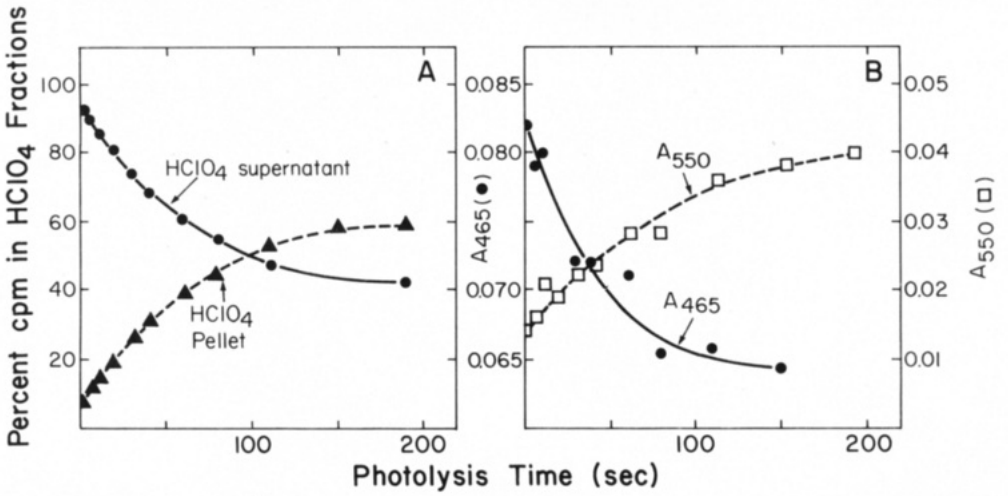

FIGURE 8: Photoincorporation of trapped [β-^{32}P]NANDP into SF_1. SF_1 (15 μM) was cross-linked with Co(phen) in the presence of 0.5 mM [β-^{32}P]NANDP (7700 cpm/nmol) and purified as described in Table II. The purified enzyme complex contained 0.87 NANDP per SF_1. Panel A: Percent cpm present in $HClO_4$-treated fractions of the [β-^{32}P]NANDP·SF_1 complex as a function of photolysis time. Co(phen) [β-^{32}P]NANDP·SF_1 (16 μM) was photolyzed in KCl–Tris buffer, pH 8.0 at 0 °C, as described under Materials and Methods. At times indicated 0.5-mL sample aliquots were precipitated by addition of 0.05 mL of 70% $HClO_4$ and centrifuged in a Beckman microfuge. The protein pellet was washed by suspension in 0.5 mL of H_2O and recentrifugation. The percent of NANDP in the combined supernatants (●) and $HClO_4$ protein pellet (▲) is shown as a function of photolysis time. Panel B: Change in the absorbance at 465 (●) and 550 nm (□) during photolysis of Co(phen) MgNANDP·SF_1 before $HClO_4$ treatment.

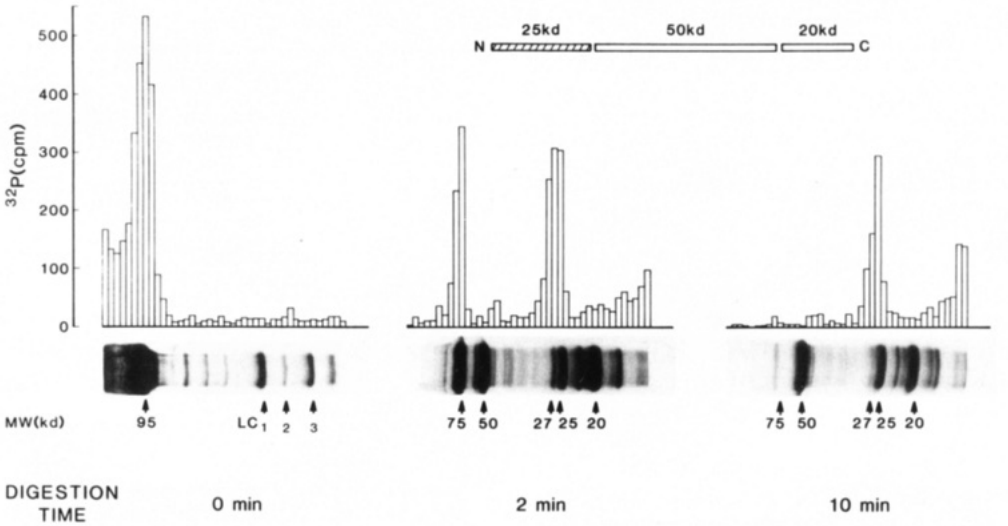

FIGURE 9: Sodium dodecyl sulfate–polyacrylamide gel electrophoresis (SDS–PAGE) analysis of a tryptic digest of NANDP-labeled SF_1. [β-^{32}P]NANDP was trapped at the active site of SF_1 (2 mg/mL) by cross-linking SH_1 and SH_2 by using the Co(phen) system. Free NANDP was removed by an ammonium sulfate precipitation of SF_1 followed by Sephadex G-25 gel filtration. After photolysis of the SF_1 for 2 min at 4 °C, the Co^{III}(phen) cross-link was reduced with Fe^{II}EDTA and the labeled SF_1 purified by ammonium sulfate precipitation and gel filtration. The labeled SF_1 (0.48 mol of covalently bound NANDP) was digested with TPCK–trypsin (1/100 w/w) for 2 and 10 min at 25 °C in 0.1 M KCl and 50 mM Tris hydrochloride (pH 8.0). The digestion was stopped by addition of a 2-fold excess of soybean trypsin inhibitor. SF_1 samples (75 μg) were analyzed on 12% acrylamide gels by using the buffer system of Laemmli (1970). ^{32}P in the gels was determined on 1.5 × 1.0 × 10 mm slices, which were mixed in 5 mL of ACS scintillant and soaked overnight before counting.

of DTNB over SF_1 (Wells & Yount, 1980). The trapped complex was purified and photolyzed for 150 s as described under Materials and Methods. The protein disulfide was reduced by treatment with dithioerythritol (DTE), the labeled enzyme was purified as above, and its ^{32}P content, its ATPase activity, and the ATP-induced increase in tryptophan fluorescence were measured. Table IV shows that in both samples the amount of recovered ATPase activity, 55% and 54%, correlated extremely well with the amount of unmodified enzyme, 58% and 61%, predicted by the extent of covalent labeling found, 42% and 39%, respectively. In addition, the inhibition of the characteristic ATP-induced fluorescence increase (Werber et al., 1972), 53% and 46%, agreed reasonably well with the extent of NANDP incorporation. The most likely explanation for these results is that the covalently incorporated NANDP was blocking access of ATP to the active site.

Localization of the Site(s) of [β-^{32}P]NANDP Photoincorporation. A procedure similar to that employed by Szilagyi et al. (1979) was used to locate the site of [β-^{32}P]NANDP incorporation within the set of partial tryptic peptides. [β-^{32}P]NANDP was trapped by Co(phen) and subsequently photolyzed as described in Figure 9. The Co(phen) modification was reversed by Fe^{II}EDTA reduction (Wells et al., 1979) to allow removal of the cross-linking Co^{III}(phen) complex and release of nonphotoincorporated NANDP. Following gel filtration the enzyme derivative was treated with trypsin for 0, 2, and 10 min (Balint et al., 1978) and analyzed by sodium dodecyl sulfate (SDS) gel electrophoresis. The stained gel (Figure 9) shows the typical cleavage pattern of first converting the heavy chain 95-kDa fragment of SF_1 into an NH_2-terminal 75-kDa piece and a carboxyl-terminal 20-kDa fragment (Balint et al., 1978; Cardinaud, 1979). The 75-kDa

Table IV: Correlation of ATPase Activity and SF_1 Tryptophan Fluorescence with the Extent of Photolabeling by Trapped [β-^{32}P]NANDP[a]

	variable measured	expt no. I (%)	expt no. II (%)
1	[β-^{32}P]NANDP trapped/SF_1	79	62
2	[β-^{32}P]NANDP photoincorporated/SF_1[b]	42	39
3	NH_4^+-EDTA ATPase activity recovered[b]	55	54
4	increase in Trp fluorescence (+ATP)[b]		
	SF_1	32	26
	NANDP-labeled SF_1	15	14
	inhibition of enhancement	53	46

[a] [β-^{32}P]NANDP was trapped on SF_1 by using a 2-fold excess of DTNB over SF_1 as described (Wells & Yount, 1980, 1982). The cross-linked complex was purified as described in Figure 9 and the [β-^{32}P]NANDP/SF_1 determined. [b] The cross-linked complex was photolyzed for 150 s (see Materials and Methods) and then treated with a 50-fold excess of DTE for 4 h at 0 °C to reduce the protein disulfide. This treatment allowed untrapped, photolyzed NANDP to be removed by $(NH_4)_2SO_4$ precipitation and gel filtration (see Table II). The [β-^{32}P]NANDP covalently attached and the ATPase activity recovered were measured (lines 2 and 3). ATP (150 μM) induced enhancement of tryptophan fluorescence was measured on SF_1 or NANDP-labeled SF_1 (15–17 μM) in 18 mM $MgCl_2$, 80 mM KCl, and 50 mM Tris, pH 7.5 at 25 °C, with a Perkin-Elmer MPF-3 fluorometer (excitation wavelength = 295 μm; emission wavelength = 334 μm).

fragment was then cleaved to an NH_2-terminal 25-kDa fragment and a 50-kDa fragment. Radiochemical analyses showed that essentially all of the photoincorporated [β-^{32}P]-NANDP was found initially in the 95-kDa heavy chain and none in the light chains. With trypsin treatment the radioactivity first appeared in the 75-kDa tryptic fragment and then in the NH_2-terminal 25-kDa fragment. With longer time the ^{32}P label appears in a 6–7-kDa fragment that runs near the dye front.

Discussion

The new ATP analogue NANTP was designed to place the photolabile nitroaryl azide group at approximately the same distance from the phosphate groups as the adenine ring is in ATP. Myosin is known to be a highly nonspecific enzyme, cleaving the terminal phosphates of essentially all triphosphate derivatives. It was felt that if NANTP bound to myosin in a productive manner then amino acids at the purine binding site could be photolabeled and identified. Another advantage was that the analogue could be easily synthesized by established procedures in both nonlabeled and radiolabeled forms from commercially available intermediates. Finally, it was thought that if the photolabeling was nonspecific, for whatever reason, we had a good chance to increase this specificity by trapping the diphosphate derivative NANDP at the active site by thiol cross-linking agents. We have previously shown that thiol cross-linking will decrease the off-rate of divalent metal ion–diphosphate complexes (e.g., MgADP) from the active site of myosin by a factor of 10^4 (Wells & Yount 1979, 1982; Wells et al., 1980c). This slow off-rate means it is possible to purify cross-linked and trapped complexes free of extraneous nucleotides before photolysis, ensuring the specificity of labeling. As will be discussed later, this was an essential step in this study.

It was first important to establish that NANTP bound to myosin in a productive manner. As shown in Table I, the kinetics of hydrolysis of NANTP by SF_1 in the presence of various metal ions were remarkably similar to those observed with ATP. Of greatest interest was the stimulation of MgNANTP hydrolysis by actin. This indicated that the rate-limiting step was the release of NANDP, a situation comparable to that seen in MgATP cleavage where the release of MgADP is rate limiting. Further verification for the similarity between ADP and NANDP binding to myosin was seen in direct binding studies. These studies (Figure 3) showed NANDP bound to SF_1 with an affinity ($K_A = 10^6$ M^{-1}) essentially identical with that measured previously for ADP (Watterson et al., 1983). In experiments to be reported elsewhere (R. Bridenbaugh, G. Kerrick, K. Nakamaye, and R. Yount, unpublished results) NANTP is shown to support tension development and relaxation of chemically skinned muscle fibers in a manner exactly analogous to that of ATP. All these results suggest that NANTP binds to myosin's active site in a productive manner.

The observation that NANTP and NANDP bound to myosin in a manner similar to ATP and ADP suggested that the NAN chromophore (under conditions of low light) might be an effective probe of the polarity of the purine binding site. Two factors favored this application: (i) the UV–visible spectra of NAN derivatives were shown not to be dependent on pH, and (ii) their absorption maxima shifted linearly 14 nm with a change in the polarity of pure solvents or mixtures of solvents. The results presented here show the λ_{max} for NANDP shifts from 474 nm in H_2O to 467 nm on binding to SF_1. This latter λ_{max} corresponds to that observed for NANDP in 40:60 H_2O:ethanol mixtures, a solution whose dielectric constant $\approx$ 45 (Landolt-Bornstein, 1959). This finding is consistent with previous results obtained with fluorescent analogues of ATP (Onodera & Yagi, 1971; Haugland, 1975; Hiratsuka, 1976; Miyata & Asai, 1982; Perkins et al., 1984) which indicated that the purine binding site of myosin was hydrophobic and was of comparable polarity to that observed here. The reasonably large molar absorptivity ($\sim$5000 M^{-1} cm^{-1}), the large shift in λ_{max} in response to solvent polarity changes, and the pH independence of the spectral changes all indicate that NAN derivatives should be useful as polarity probes of binding sites on other enzymes.

The above results all indicated that NANTP and NANDP were binding tightly and that they were binding in the correct orientation to the active site of myosin. It was surprising then to find that NANDP was ineffective in photoinactivating SF_1 unless large excesses of analogue were present. Moreover, the addition of ATP or AMP-PNP had no effect on the inactivation, indicating that the activity-critical amino acid residues being modified were not at the active site. Fortunately, it was found possible to stabilize the binding of NANDP to the active site by cross-linking two thiols (believed to be SH_1 and SH_2) with a variety of different bifunctional reagents (Table II). Trapped NANDP was remarkably stable ($\tau_{1/2}$ was >5 days at 0 °C), and the cross-linked trapped complex could be purified free of nontrapped NANDP by conventional $(NH_4)_2SO_4$ precipitation and gel filtration. The approximately equal stoichiometry of trapped Mg and NANDP to SF_1 active sites and the enhanced rate of Co(phen) inactivation by addition of MgNANDP all indicated that trapping was specific and was at the active site. In addition, AMP-PNP would not bind to the cross-linked trapped complex. These results meant that photoincorporation would now be specific and the location of the purine binding site could be determined.

Accordingly, photolysis studies on the purified NANDP·SF_1 complex cross-linked by Co^{III}(phen), by pPDM, or by oxidation with DTNB all gave >60% covalent labeling of SF_1 by the trapped analogue. Since the cross-linked trapped complexes contained only 0.65–0.87 NANDP/SF_1, overall, some 40–50% of the total active sites were labeled. This high-percentage incorporation may result from the increased residence time

that cross-linking has given the photoactivated NANDP. The incorporation (>95%) was all in the heavy chains. This result is consistent with recent findings (Wagner & Giniger, 1981; Sivaramakrishnan & Burke, 1982) that the heavy chains alone, free of light chains, contained the actin-activated ATPase activity. Subsequent limited trypsin treatment and SDS gel electrophoretic analysis placed the purine binding site in the NH_2-terminal 25-kDa heavy chain fragment. Little or no labeling occurred in the 20-kDa or 50-kDa tryptic peptides or the light chains. The location of the active site in the NH_2-terminal 25-kDa tryptic peptide had previously been suggested by the photoaffinity labeling studies of Szilagyi et al. (1979). These workers used the ATP analogue introduced by Jeng & Guillory (1975) in which a (nitroaryl)azido group is linked via β-alanyl to the 3'-OH of ATP. In this case the photogenerated nitrene group is some 10 Å from the 3'-oxygen of ATP, and because the β-alanyl linker is flexible, it is possible that the nitrene labels residues not directly involved with the active site. Regardless, the results of this study as well as the results reported here place at least part of the active site toward the NH_2-terminal end of the myosin heavy chain. It is worth noting that other recent photoaffinity labeling studies of myosin with 3'-*O*-(4-benzoyl)benzoyl-ATP (Mahmood & Yount, 1984) place part of the 50-kDa fragment at or near the active site. Thus it is likely that portions of both the 25-kDa and 50-kDa peptides contribute to the active site and that it is premature to think of the 25-kDa fragment as the "nucleotide binding domain". Nonetheless, it is now clear with reasonable certainty that the purine binding site exists in the 25-kDa fragment.

Finally, this study illustrates the advantage of the use of cross-linking agents to stabilize binding of photoprobes at the active site. This technique may be of use in studies of other enzymes that undergo substantial substrate-induced conformation changes. The resulting increased stability (i) allows the photoprobe complex to be purified *before* photolysis and (ii) increases the residence time of the reactive photoproduct. As a consequence, the specificity and extent of photolabeling is enhanced. Both of these goals were attained in this study and in work reported elsewhere (Okamoto & Yount, 1985); we have established that the majority of photolabeling occurs with a specific tryptophan residue in the heavy chain. Clearly none of this would have been possible without the discovery of the trapping phenomena since, as shown here, extensive nonspecific labeling occurred in the absence of cross-linking. This general approach is currently being extended with a variety of other ATP photoaffinity analogues with the plan to place specific amino acid residues at precise locations about the ATP binding site. Such information should be of considerable usefulness in positioning ATP in the context of the overall crystal structure of SF_1 (Rayment & Winkelmann, 1984).

ACKNOWLEDGMENTS

We are indebted to Jean Grammer, Mary Shelton, and Catherine Knoeber for their technical assistance and to Margaret Kelnhofer for her aid in the preparation of the manuscript. Charles Mahoney developed the HPLC system used to separate the various NAN derivatives. Harvey Penefsky suggested the use of NANTP as a substrate for F_1-ATPase and generously provided the enzyme we used.

REFERENCES

Ablov, A. V., & Palade, D. M. (1961) *Russ. J. Inorg. Chem.* (*Engl. Transl.*) *6*, 306.

Balint, M., Wolf, I., Tarcsafalvi, A., Gergley, J., & Sreter, F. A. (1978) *Arch. Biochem. Biophys. 190*, 793.

Bradford, M. M. (1976) *Anal. Biochem. 72*, 248.

Cardinaud, R. (1979) *Biochimie 61*, 807.

Fleet, G. W. J., Porter, R. R., & Knowles, J. R. (1969) *Nature* (*London*) *224*, 51.

Gresser, M. J., Myers, J. A., & Boyer, P. D. (1982) *J. Biol. Chem. 257*, 12030.

Guillory, R. J., & Jeng, S. J. (1977) *Methods Enzymol. 46*, 259.

Haley, B. E., & Yount, R. G. (1972) *Biochemistry 11*, 2863.

Haugland, R. P. (1975) *J. Supramol. Struct. 3*, 338.

Hoard, D. E., & Ott, D. G. (1965) *J. Am. Chem. Soc. 87*, 1785.

Jeng, S. J., & Guillory, R. J. (1975) *J. Supramol. Struct. 3*, 448.

Kosower, E. M. (1958) *J. Am. Chem. Soc. 80*, 3253.

Laemmli, U. K. (1970) *Nature* (*London*) *227*, 680.

Landolt-Bornstein, H. H. (1959) *Zahlenwerte und Funktionen*, 6th ed., p 613, Springer-Verlag, Berlin, West Germany.

Laskey, R. A., & Mills, A. D. (1975) *Eur. J. Biochem. 56*, 335.

Mahmood, R., & Yount, R. G. (1984) *J. Biol. Chem. 259*, 12956.

Miyata, H., & Asai, H. (1982) *Biochem. Biophys. Res. Commun. 105*, 296.

Okamoto, Y., & Yount, R. G. (1985) *Proc. Natl. Acad. Sci. U.S.A. 82*, 1575.

Onodera, M., & Yagi, K. (1971) *Biochim. Biophys. Acta 253*, 254.

Ott, D. G., Kerr, V. N., Hansbury, E., & Hayes, E. N. (1967) *Anal. Biochem. 21*, 469.

Rayment, I., & Winkelmann, D. A. (1984) *Proc. Natl. Acad. Sci. U.S.A. 81*, 4378.

Sivaramakrishnan, M., & Burke, M. (1982) *J. Biol. Chem. 257*, 1102.

Spudich, J., & Watt, S. (1971) *J. Biol. Chem. 246*, 4866.

Szilagyi, L., Balint, M., Sreter, F. A., & Gergely, J. (1979) *Biochem. Biophys. Res. Commun. 87*, 936.

Togashi, C. J., & Reisler, E. (1982) *J. Biol. Chem. 257*, 10112.

Tong, S. W., & Elzinga, M. (1983) *J. Biol. Chem. 258*, 13100.

Turner, D. C., & Brand, L. (1968) *Biochemistry 7*, 3381.

Wagner, P. D., & Yount, R. G. (1975) *Biochemistry 14*, 1900.

Wagner, P. D., & Yount, R. G. (1976) *J. Biol. Chem. 251*, 5424.

Wagner, P. D., & Weeds, A. G. (1977) *J. Mol. Biol. 109*, 445.

Wagner, P. D., & Giniger, E. (1981) *Nature* (*London*) *292*, 560.

Watterson, J. G., Foletta, D., Kunz, P. A., & Schaub, M. C. (1983) *Eur. J. Biochem. 131*, 89.

Weeds, A. G., & Taylor, R. S. (1975) *Nature* (*London*) *257*, 54.

Wells, J. A., & Yount, R. G. (1979) *Proc. Natl. Acad. Sci. U.S.A. 76*, 4966.

Wells, J. A., & Yount, R. G. (1980) *Biochemistry 19*, 1711.

Wells, J. A., & Yount, R. G. (1982) *Methods Enzymol. 85*, 93.

Wells, J. A., Werber, M. M., Legg, J. I., & Yount, R. G. (1979) *Biochemistry 18*, 4793.

Wells, J. A., Sheldon, M., & Yount, R. G. (1980a) *J. Biol. Chem. 255*, 1598.

Wells, J. A., Werber, M. M., & Yount, R. G. (1980b) *J. Biol. Chem. 255*, 7552.

Wells, J. A., Knoeber, C., Sheldon, M. C., Werber, M. M., & Yount, R. G. (1980c) *J. Biol. Chem. 255*, 11135.

Werber, M. M., Szent-Gyorgyi, A. G., & Fasman, G. D. (1972) *Biochemistry 11*, 2872.
Werber, M. M., Oplatka, A. & Danchin, A. (1974) *Biochemistry 13*, 2683.
Yoshikawa, M., Kato, T., & Takenishi, T. (1967) *Tetrahedron Lett.*, 5065.
Yount, R. G., Babcock, D., Ballantyne, W., & Ojala, D. (1971) *Biochemistry 10*, 2484.

Kinetic Mechanisms of Two NAD:Arginine ADP-Ribosyltransferases: The Soluble, Salt-Stimulated Transferase from Turkey Erythrocytes and Choleragen, a Toxin from *Vibrio cholerae*

James C. Osborne, Jr.,*,‡ Sally J. Stanley,§ and Joel Moss§
Molecular Disease Branch and Laboratory of Cellular Metabolism, National Heart, Lung, and Blood Institute, National Institutes of Health, Bethesda, Maryland 20205
Received November 28, 1984

ABSTRACT: A subunit of choleragen and an erythrocyte ADP-ribosyltransferase catalyze the transfer of ADP-ribose from NAD to proteins and low molecular weight guanidino compounds such as arginine. These enzymes also catalyze the hydrolysis of NAD to nicotinamide and ADP-ribose. The kinetic mechanism for both transferases was investigated in the presence and absence of the product inhibitor nicotinamide by using agmatine as the acceptor molecule. To obtain accurate estimates of kinetic parameters, the transferase and glycohydrolase reactions were monitored simultaneously by using [*adenine*-2,8-^{3}H]NAD and [*carbonyl*-^{14}C]NAD as tracer compounds. Under optimal conditions for the transferase assay, NAD hydrolysis occurred at <5% of the V_{max} for ADP-ribosylation; at subsaturating agmatine concentrations, the ratio of NAD hydrolysis to ADP-ribosylation was significantly higher. Binding of either NAD or agmatine resulted in a greater than 70% decrease in affinity for the second substrate. All data were consistent with a rapid equilibrium random sequential mechanism for both enzymes.

ADP-ribosylation is a covalent modification in which the ADP-ribose moiety of NAD is transferred to specific proteins (reaction 1) (Hayaishi & Ueda, 1977; Vaughan & Moss, 1982; Pekala & Moss, 1983). Several amino acids can serve as ADP-ribose acceptors; among these are arginine (Goff, 1974; Moss & Vaughan, 1977, 1978; Moss & Richardson, 1978), glutamate (Riquelme et al., 1979; Burzio et al., 1979; Ogata et al., 1980a,b), asparagine (Manning et al., 1984), and diphthamide (Van Ness et al., 1980a,b), a posttranslationally modified histidine residue. These ADP-ribosyltransferases also catalyze the hydrolysis of NAD to ADP-ribose and nicotinamide (reaction 2) (Moss & Vaughan, 1978; Kandel et al., 1974; Moss et al., 1976, 1983; Ueda et al., 1975; Katada et al., 1983). The presence of this abortive reaction indicates that the transferases are capable of activating the ribosyl–nicotinamide bond in the absence of an amino acid or protein acceptor. It is possible that binding of the ADP-ribose acceptor requires the initial binding of NAD (ordered sequential mechanism) or that, in fact, both substrates bind independently (random sequential mechanism). Chung & Collier (1977) have investigated the kinetics of interaction of NAD and the ADP-ribose acceptor with diphtheria toxin. This bacterial toxin is a member of one class of ADP-ribosyltransferases that catalyzes the ADP-ribosylation of a modified histidine residue in elongation factor II (Van Ness et al., 1980a,b), thereby inhibiting protein synthesis (Chung & Collier, 1977). These investigators presented a model in which NAD binding must precede the binding of elongation factor II (EF-2) (reactions 3a,b) (Chung & Collier, 1977). The formation of a ternary complex, i.e., enzyme–NAD–acceptor, is supported by the finding that all ADP-ribosyltransferases appear to be stereospecific (Ferro & Oppenheimer, 1978; Oppenheimer, 1978; Moss et al., 1979a,b; Oppenheimer & Bodley, 1981); the enzymes use β-NAD as a substrate and, in the presence of an acceptor, form the α-anomeric product.

$$\text{NAD} + \text{protein} \rightarrow \text{ADP-ribose protein} + \text{nicotinamide} + \text{H}^+ \quad (1a)$$

$$\text{NAD} + \text{amino acid} \rightarrow \text{ADP-ribose–amino acid} + \text{nicotinamide} + \text{H}^+ \quad (1b)$$

$$\text{NAD} + \text{H}_2\text{O} \rightarrow \text{ADP-ribose} + \text{nicotinamide} + \text{H}^+ \quad (2)$$

$$\text{enzyme} + \text{NAD} \rightleftharpoons \text{enzyme–NAD} \quad (3a)$$

$$\text{enzyme–NAD} + \text{EF-2} \rightleftharpoons \text{enzyme–NAD–EF-2} \rightarrow \text{products} \quad (3b)$$

A subclass of ADP-ribosyltransferases uses free arginine, in addition to proteins, as ADP-ribose acceptors (Moss & Vaughan, 1977, 1978; Moss & Richardson, 1978). Included in this group of enzymes are choleragen (cholera toxin) (Moss & Vaughan, 1977) and *Escherichia coli* heat-labile enterotoxin (Moss & Richardson, 1978), the bacterial toxins responsible for the activation of adenylate cyclase in animal cells (Moss & Vaughan, 1981), and erythrocyte NAD:arginine ADP-ribosyltransferases (Moss & Vaughan, 1978). We have examined the kinetics of the transferase reaction with two of these enzymes, cholera toxin (CT)[1] and erythrocyte transferase (ET). The studies support a model clearly different from that

‡ Molecular Disease Branch.
§ Laboratory of Cellular Metabolism.

[1] Abbreviations: CT, choleragen (cholera toxin); ET, erythrocyte transferase.